

Synthesis of Selective Bioactive Pyridylpyridones: *in silico* Studies and Biological Evaluations

SURESH RAMASAMY^{1,2}, SINGANAN PONNUCHAMY^{1,*} and SIVAKUMAR PONNUSAMY²

¹Alivira Animal Health Ltd, R & D Center, Visakhapatnam-530019, India

²Department of Chemistry, Arignar Anna Government Arts College, Namakkal-637002, India

*Corresponding author: E-mail: ponnuchamy_85@yahoo.co.in

Received: 24 June 2019;

Accepted: 18 August 2019;

Published online: 29 April 2020;

AJC-19824

Twenty three substituted pyridylpyridones were designed and performed for molecular docking studies against α -amylase enzyme. The top three hit molecules were synthesized and characterized by ¹H NMR, ¹³C NMR, ESI-mass and FT-IR spectroscopic techniques. Experimental biological applications were studied for these compounds. The DFT calculations were executed for the hit compounds. In addition, molecular electrostatic potential mapping was also executed for additional support.

Keywords: Pyridines, Anti-diabetic, Molecular docking, DFT studies, Molecular electrostatic map potential.

INTRODUCTION

Many heterocyclic compounds are originated by plants which showed numerous biological applications [1,2]. Especially, *N*-heterocyclic compounds have attracting biological and pharmacological properties [3]. Among various nitrogen containing heterocycles, 2-pyridone has a number of applications which is intermediate to the synthesis of the biologically active pyridine, quinoline, quinolizidine and indolizidine and also simple pyridones itself demonstrated as a bioactive compound [4]. In recent years, pyridones and its derivatives have a significant interest in the field of drug discovery. For example, the pyridone containing compounds showed multiple biological activities such as anti-inflammatory [5], antifungal [6], anti-bacterial [7] and antioxidant activities [8].

Similarly, pyridone based compounds such as milrinone and amrinone are used as cardiotonic agents [9]. Also, the researchers found that the ring-fused 2-pyridones act as acetylcholinesterase inhibitors [10], PARP-1 inhibitors [11] (PJ34) and anti-HIV agents [12]. Although Xu *et al.* [13] suggested that pyridone derivatives exhibited anticancer activity against lung cancer cells. Based on the prominence of pyridone, the research is motivated to synthesize pyridyl pyridone derivatives.

Molecular docking has been demonstrated a very efficient tool for novel drug discovery for targeting protein and most

frequently used methods in structure-based drug design [14, 15]. It is generally known that molecular binding of one molecule (ligand) to the pocket of another molecule (receptor) [16]. This is a quicker and inexpensive method to identify drug candidates [17]. The major advantage of molecular docking is used to reduce the number of synthetic compounds in the field of drug discovery.

Structure activity relationship (SAR) is helping to understand the chemical-biological interactions in drug discovery research. SAR is useful to design the library of compound targeted toward particular receptors to increase the therapeutically active drug. Herein, 23 pyridone derivatives were screened for molecular docking studies. Out of 23 molecules, top three molecules are planning to synthesize because they may have good inhibitory activity. In continuation, experimental biological applications are planning to study for these compounds. DFT studies play an important role [18] in the identification of the properties of compounds under investigations, like HOMO, LUMO, band gap, chemical potential, electronegativity, global hardness and softness and electrophilicity index [19]. The comparative experimental and computational results give more information for biological studies [20]. The DFT calculations and molecular electrostatic potential are also focused to evaluate for the synthesized compounds.

EXPERIMENTAL

All the solvents used were analytical grade and purchased from Spectrochem and Sigma-Aldrich. Reactions were monitored by TLC analysis on precoated silica gel 60 F₂₅₄ in TLC sheets (0.2 mm thickness, Merck plate) and 60-120 mesh Merck silica gel used for column chromatography. Petroleum ether and ethyl acetate were used as the eluents. ¹H- and ¹³C-NMR spectra were recorded on Bruker 500 MHz and 125 MHz instruments, CDCl₃ and DMSO-*d*₆ were used as an internal solvent; δ in ppm relative to Me₄Si as internal standard, *J* in Hz. ESI-MS spectra were recorded in LCQ fleet mass spectrometer. FT-IR spectra were recorded in Thermo Scientific Nicolet iS50 FT-IR Spectrometer. Absorption measurements were carried out using a JASCO-V630 spectrophotometer (for α-amylase study).

General procedure for the synthesis of pyridone derivatives: To an ethanolic solution (10 mL) of acetyl pyridine (8.26 mmol), ethyl cyanoacetate (8.26 mmol), corresponding aldehyde (8.26 mmol) and ammonium acetate (66.08 mmol) was added. The reaction mixture was refluxed for 1-6 h. The completion of the reaction was monitored by thin layer chromatography. Then the reaction mixture was poured into crushed ice and filtered. The filtered solid was dried and purified by column chromatography using dichloromethane:methanol as a eluent (**Scheme-I**).

4-(2-Chlorophenyl)-6-oxo-1,6-dihydro[2,4'-bipyridine]-5-carbonitrile (3c): ¹H NMR (500 MHz, DMSO-*d*₆) δ 8.64 (d, *J* = 5.4 Hz, 2H), 7.97 (d, *J* = 5.4 Hz, 2H), 7.63 (d, *J* = 7.8 Hz, 1H), 7.53 - 7.49 (m, 2H), 7.45 (d, *J* = 8.4 Hz, 1H), 6.77 (s, 1H). ¹³C NMR (125 MHz, DMSO-*d*₆) δ 168.89, 153.40, 152.37, 148.31, 144.13, 135.56, 130.00, 129.75, 128.80, 128.07, 125.57, 119.74, 117.03, 104.00, 95.57. ESI-mass: calcd. (found): 307.05 (306.10) (M-1)⁻; IR (KBr disc, ν_{max}, cm⁻¹): 3019, 2821, 2205, 1660, 1538, 824, 762.

6-Oxo-4-phenyl-1,6-dihydro[2,3'-bipyridine]-5-carbonitrile (3f): ¹H NMR (500 MHz, DMSO-*d*₆) δ 13.08 (s, 1H), 9.14 (s, 1H), 8.78 (d, *J* = 4.7 Hz, 1H), 8.36 (d, *J* = 8.1 Hz, 1H), 7.87-7.80 (m, 2H), 7.70-7.59 (m, 3H), 7.05 (s, 1H). ¹³C NMR (125 MHz, DMSO-*d*₆) δ 160.38, 158.57, 153.96, 152.38, 143.27, 137.96, 130.09, 128.79, 120.08, 118.10, 112.57, 105.35, 99.20, 91.43. ESI-mass: calcd. (found): 273.09 (272.18) (M-1)⁻; IR (KBr disc, ν_{max}, cm⁻¹): 3069, 2973, 2211, 1661, 1551, 809, 760.

4-(2,5-Difluorophenyl)-6-oxo-1,6-dihydro-[2,3'-bipyridine]-5-carbonitrile (3g): ¹H NMR (500 MHz, DMSO-*d*₆) δ 9.15 (s, 1H), 8.62 (bs, 1H), 8.37 (d, *J* = 8.0 Hz, 1H), 7.55-7.50 (m, 1H), 7.44-7.39 (m, 3H), 6.82 (s, 1H). ¹³C NMR (126 MHz, DMSO-*d*₆) δ 171.27, 159.94, 158.05, 157.21, 156.78, 154.76, 150.77, 150.08, 148.92, 135.66, 135.00, 124.84, 120.05, 118.73, 118.46, 117.88, 105.52, 95.67. ESI-mass: calcd. (found): 309.07 (309.85) (M+1)⁺; IR (KBr disc, ν_{max}, cm⁻¹): 3169, 2963, 2205, 1657, 1534, 819, 725.

α-Amylase inhibition activity

α-Amylase inhibition assay was carried out by the reported literature [21]. In brief, various concentrations of synthesized compounds and acarbose solution were prepared in phosphate buffer (pH = 6.9, 0.2 M). To that solution, 0.5 % of α-amylase in phosphate buffer was added. The mixture was incubated

for 10 min at 37 °C. Then a 1% starch solution was added and incubated for 30 min at 37 °C. To that mixture, 3,5-dinitrosalicylic acid (DNSA) reagent was added to stop the enzymatic reaction and incubated in boiling water bath for 15 min. Then the absorbance measured at 540 nm on a spectrophotometer. From the absorbance results, the % inhibition was calculated as follows:

$$\text{Inhibition (\%)} = \frac{A_t - A_c}{A_t} \times 100$$

where, A_t = O.D. of test solution, A_c = O.D. of control.

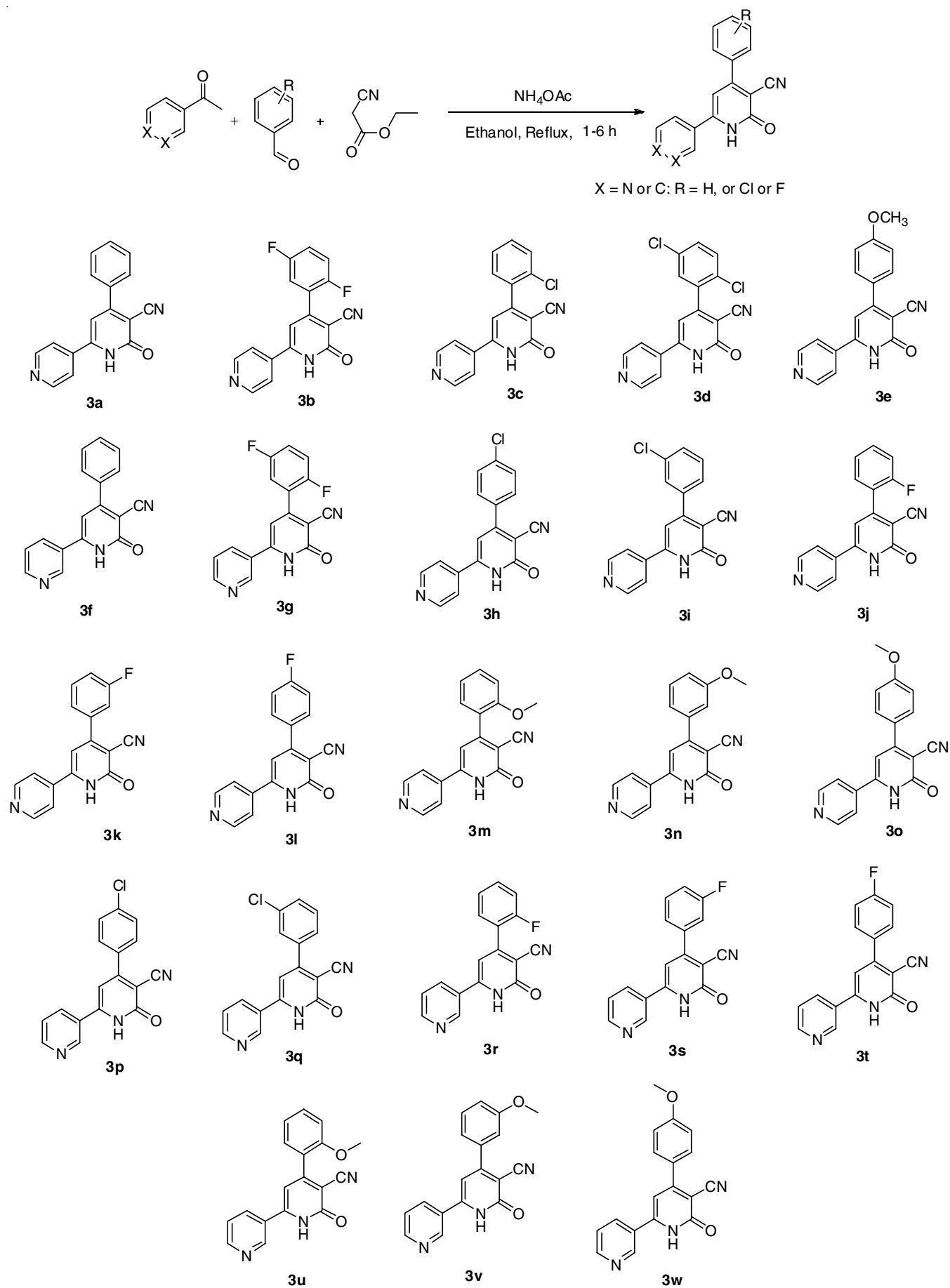
Molecular docking study: Molecular docking of compounds was carried out with α-amylase enzyme. Autodock 4.2 software was used for docking studies [22]. Three dimensional structure of synthesized compounds (**3a-w**) were constructed using ChemBio 3D ultra 13.0 software and then they were energetically minimized using MMFF94 (number of interaction is 5000, RMS gradient is set as 0.10) [23]. The crystal structure of the enzyme (PDB ID: 1HNY) was taken from Protein Data bank (www.rcsb.org). The docked complexes were visualized using discovery studio 4.1 client.

Computational calculations: Computational calculations of highest occupied molecular orbital (HOMO) and lowest unoccupied molecular orbital (LUMO) in the checkpoint files were performed with Gaussian 09 W program using DFT methods [24]. The three dimensional structures of the compounds were optimized with B3LYP/6.311 ++ G (d,p) basis set. The Gauss view software package was used to visualize the computed structures including HOMO, LUMO and molecular electrostatic potential (MEP) representations.

RESULTS AND DISCUSSION

The top three hit compounds (**3c**, **3f** and **3g**) from molecular docking results were synthesized. The corresponding aldehydes react with 4-pyridyl acetophenone/3-pyridyl acetophenone and ethyl cyanoacetate in the presence of ammonium acetate under reflux condition yielded the target compounds. The reaction was carried out by one-pot synthetic method. The ethanol is used as a solvent and the reaction time was 1-6 h.

The synthesized compounds were characterized using spectroscopic techniques. In ¹H NMR clearly showed the singlet at around 6.7 ppm which is appeared for pyridone C5 attached proton. It confirms the formation of pyridone unit. The peaks appeared at 8.6, 7.9 ppm in compound **3c** and 9.1 to 8.3 ppm in compounds **3f** and **3g** indicates the presence of pyridyl ring. The remaining protons appeared for aryl units. Similarly, the ¹³C NMR also confirms the product formation. The carbon signal in the region of 90-96 ppm indicates the presence of nitrile group. The carbon signals around 168-172 ppm indicate the presence of pyridone C4 carbon. The carbon signals around 99-104 ppm appeared due to the presence of C5 pyridone carbon. The other peaks appeared for remaining carbon units. The mass spectrum also confirms the product formation. The compounds showed a molecular ion peak in either positive or negative mode. The FT-IR spectrum gave some additional information for the compounds. The absorbance around 2200 cm⁻¹ indicates the presence nitrile group which is appeared due to nitrile stretching frequencies. The peak around 1650 cm⁻¹ indicates the presence of



Scheme-I: Synthetic route of pyridylpyridones

pyridone carbonyl units. The absorbance around 3100-2800 cm^{-1} appeared for aromatic CH stretching frequencies.

Molecular docking studies

Selection and preparation of protein/enzymes structures:

Molecular docking of pyridylpyridones (**3a-w**) was carried out with α -amylase enzyme. The crystal structure of α -amylase was downloaded from the Protein Data bank (www.rcsb.org). Water and ligand molecules were excluded from the target and polar hydrogen was added to the target. α -Amylase is one of the important enzymes because it plays a key role in the breakdown of starch to glucose. Excess of glucose levels affects diabetic patients. So inhibitors of α -amylase can effectively retard the digestion as well as the significant delay of postprandial hyperglycemia [25,26]. Hence, α -amylase is considered to be one of the best targets for the development of type II diabetes therapeutic agents.

Molecular docking of α -amylase with compounds **3a-w**:

The docking of designed pyridylpyridones (**3a-w**) into the active site of α -amylase was performed and identified hit compounds exhibited favorable docking scores and interactions. Particularly, compounds **3c**, **3f** and **3g** showed better potent binding energy and inhibition constant together with more hydrogen interactions than other derivatives. The docking results are represented in Table-1 and molecular docking interactions of hit compounds are shown in Fig. 1.

Molecular docking analysis of compound **3c** in 1HNY:

The docking pose of compound **3c** in the active site of 1HNY was given in its three dimensional mode. The docking pose analysis revealed that pyridylpyridone is oriented in π -alkyl and π -sigma interactions surrounded by the amino acid side chains of Ala198, Leu162 and Trp59 in the active site of 1HNY. Five hydrogen bond interactions, one being between C=O group of compound **3c** and imidazolyl nitrogen present in the residue

TABLE-1
MOLECULAR DOCKING INTERACTION OF THE PYRIDYLPYRIDONES (**3a-w**) AGAINST α -AMYLASE

Compound No.	Binding energy (Kcal/mol)	Inhibition constant (μM)	Number of hydrogen bonding	Interacted amino acid residue (1HNY)
3a	-6.14	31.75	2	LYS200, GLU233
3b	-6.54	16.16	5	GLU233, ARG195, ASP197, HIS299, TYR62
3c	-7.72	2.2	5	ASP197, GLU233, ARG195, ASP300, HIS299
3d	-6.14	31.75	3	ASP300, ARG195, HIS101
3e	-6.43	19.44	5	ASP300, ARG195, ASP197, TYR62, ALA198
3f	-7.64	2.52	5	GLU233, ARG195, ASP197, HIS299, TYR62
3g	-7.45	3.42	5	HIS299, ARG195, GLU233, ASP197, ASP197
3h	-6.47	18.1	0	-
3i	-6.39	20.66	0	-
3j	-6.42	19.61	4	ARG195, ARG195, HIS101, TRP59
3k	-6.23	27.03	1	TRP59
3l	-6.36	21.80	2	HIS201, TRP58
3m	-6.54	16.14	1	HIS201
3n	-6.86	9.32	1	GLU233
3o	-6.85	9.47	5	ARG252, ARG252, ARG252, ARG252, ARG398
3p	-6.67	12.84	2	ARG195, ARG195
3q	-6.38	20.07	1	THR163
3r	-6.67	12.84	3	HIS101, ARG195, ARG195
3s	-6.39	20.85	1	HIS101
3t	-6.72	11.8	2	ARG195, ARG195
3u	-6.42	19.78	0	0
3v	-6.97	7.76	1	ASP300
3w	-6.67	12.84	3	ARG398, ARG252, ARG252

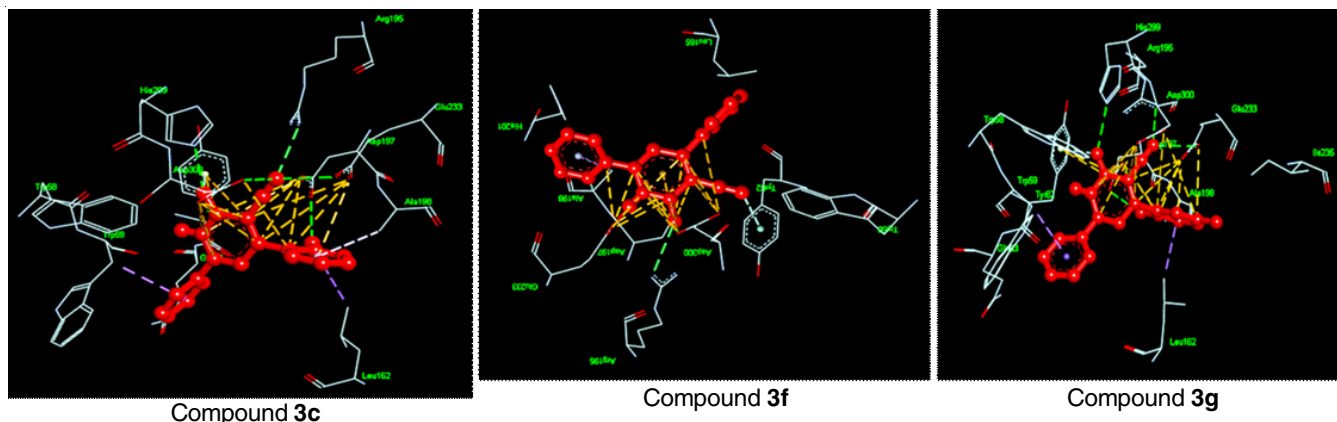


Fig. 1. Molecular docking studies of synthesized compounds (**3c**, **3f** and **3g**) against α -amylase enzymes

of His299 ($C=O \cdots N_{\text{His299}} = 2.77 \text{ \AA}$), a second H-bonding interaction between Cl group of compound **3c** and the acidic side chain of α -carboxylic acid residue in Asp197 ($\text{OH}_{\text{Asp197}} \cdots \text{Cl}_{\text{pyridone ring}} = 3.14 \text{ \AA}$). Other three hydrogen bonds were observed between the CN group of pyridone ring with amino acid residues Glu233, Arg195 and Asp300. Their bonding distance is found to be 2.90, 2.90 and 2.55 \AA . These interactions increase the binding affinity of the molecule as indicated by the docking score of the compound **3c** as -7.72 Kcal/mol and inhibitions constant is 2.2 μM .

Molecular docking analysis of compound **3f** in 1HNY:

Compound **3f** showed five hydrogen bonding interactions, H-bonding interacted amino acid residues were found to be Gly104, Gln63/Gln63 and Trp59/Trp59. And also it showed a very good binding energy (-7.64 Kcal/mol) and inhibition constant (2.52 μM). Pyridine ring of Compound **3f** has hydrogen bonding interaction with Gly104, the bond distance is found to be 3.13 \AA . A NH group of Gln63 has two hydrogen bonding interactions through pyridone ring with the bond distance of 3.00 and 3.74 \AA . Trp59 has π -donor hydrogen bond interaction with the pyridone carbonyl and nitrile. The hydrogen bonding distance is found to be 3.51 and 3.58 \AA . Further, pyridine ring has π -alkyl and π - σ interactions with the amino acid residue of Val107 and Gly104, respectively. Similarly, benzene ring has π - σ interaction with Leu165. Pyridone ring was surrounded by π - π stacked with the amino acid of Trp59.

Molecular docking analysis of compound **3g** in 1HNY:

Likewise, in case of compound **3g**, five hydrogen bond interactions were found with 1HNY enzymes. Compound **3g** has the least binding energy (-7.45 Kcal/mol) and exhibited better inhibition constant (3.42 μM). The nitrile group formed two hydrogen bonding interactions with Glu233 and Arg195, respectively. Similarly, fluoro substitutions showed two hydrogen bonding interactions with Asp197/Asp197. Another hydrogen bonding interaction was observed between the $C=O$ group of compound **3g** and imidazole nitrogen of His299. In addition, fluoro benzene ring forms π -alkyl and π - σ interactions with Ala198 and Leu162, respectively. On the other hand, the pyridine ring forms π - σ interaction with Trp59. Furthermore, carbonyl group exhibited π -donor hydrogen bond interaction with Tyr62.

Biological studies

α -Amylase inhibitory activity: The compounds **3c**, **3f** and **3g** were screened for α -amylase inhibitory activity. The α -amylase inhibitory study was carried out at different concentrations (10-200 μM). Acarbose is used as a standard to compare their inhibitions. In 10 μM concentration, standard acarbose showed 16.89 percentage inhibitions while the synthesized compounds displayed 12.45-10.89 percentage inhibition. At 25 μM concentration, compounds **3c**, **3f** and **3g** have shown 23.85 -21.22 percentage inhibition which is a nearer activity

to standard acarbose (26.95 % percentage inhibition). Synthesized compounds (**3c**, **3f** and **3g**) showed 47.70-45.01 percentage inhibitions at 50 μM concentration whereas standard has 54.78 percentage inhibitions. Again, the percentage inhibition was tested at higher concentrations such as 100 and 200 μM , particularly compound **3c** showed 62.47 and 84.33 percentage inhibition at 100 and 200 μM concentrations. At the same concentration, standard showed 65.59 and 89.41 percentage inhibition. Over all from the graphical chart of α -amylase inhibitory studies, synthesized compounds showed good inhibitory activity because the percentage inhibitions were nearer to standard drug. Moreover, compound **3c** showed good α -amylase inhibitory activity than the other two derivatives. The percentage inhibitions are shown in Fig. 2.

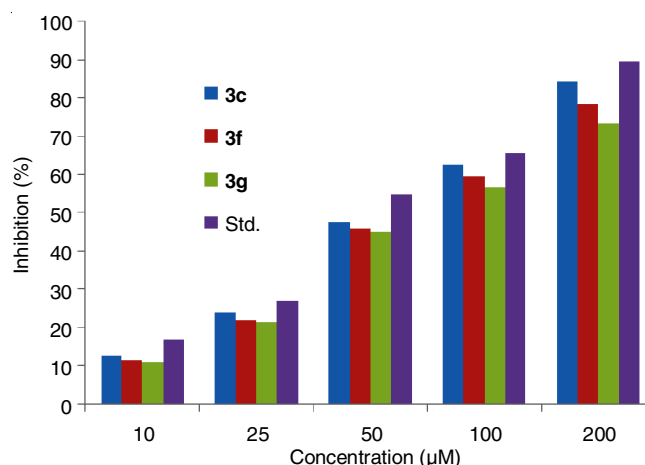


Fig. 2. α -Amylase inhibitory activity of synthesized compounds

Frontier molecular orbitals: Frontier molecular orbitals of the molecules will explain the molecule's reactivity. HOMO energy is associated with reactivity to electrophilic attack while LUMO energy is associated with reactivity to nucleophilic attack. The DFT parameters are represented in Table-2. The negative energies of HOMO and LUMO indicating the stability of the compound [27]. The band gap of HOMO and LUMO has been used to predict the molecule reactivity and stability of the molecule. The decrease energy gap explains charge transfer interaction within the molecule. The lower band gap of the molecule is a more reactive molecule which may have more bioactivity [28]. Among these synthesized compounds, compound **3c** possess lower energy gap. This may be due to the introduction of a sterically hindered Cl- group (*ortho*-substitution) in the benzene ring. The more reactive compound **3c** exposed more enzyme inhibition *in vitro* studies. The electrophilicity index is the ability to accept the electron from the environment [29]. The increasing order of electrophilicity index value is compound **3c** ($\omega = 10.6607$) > **3f** ($\omega = 4.5596$) > **3g** ($\omega = 4.9044$). The compound **3c** exhibited the highest value of electrophilicity index which

TABLE-2
DFT CALCULATIONS OF SYNTHESIZED COMPOUNDS

Compound No.	HOMO (eV)	LUMO (eV)	Band gap (ΔE)	Chemical potential	Global hardness	Global softness	Electrophilicity index
3c	-6.0973	-3.8001	2.297	-4.9487	1.1486	0.4353	10.6607
3f	-6.4579	-2.2757	4.182	-4.3668	2.0911	0.2391	4.5596
3g	-6.6146	-2.4376	4.177	-4.5261	2.0885	0.2394	4.9044

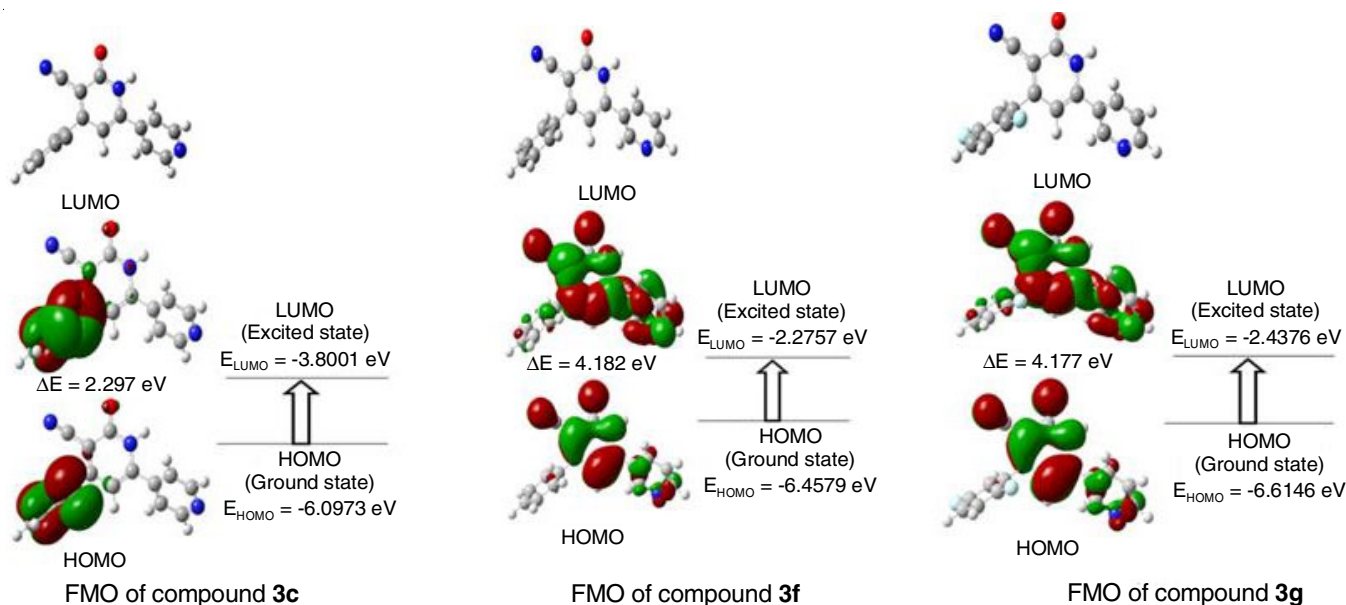
Fig. 3. Frontier molecular orbitals (FMO) of **3c**, **3f** and **3g** compounds

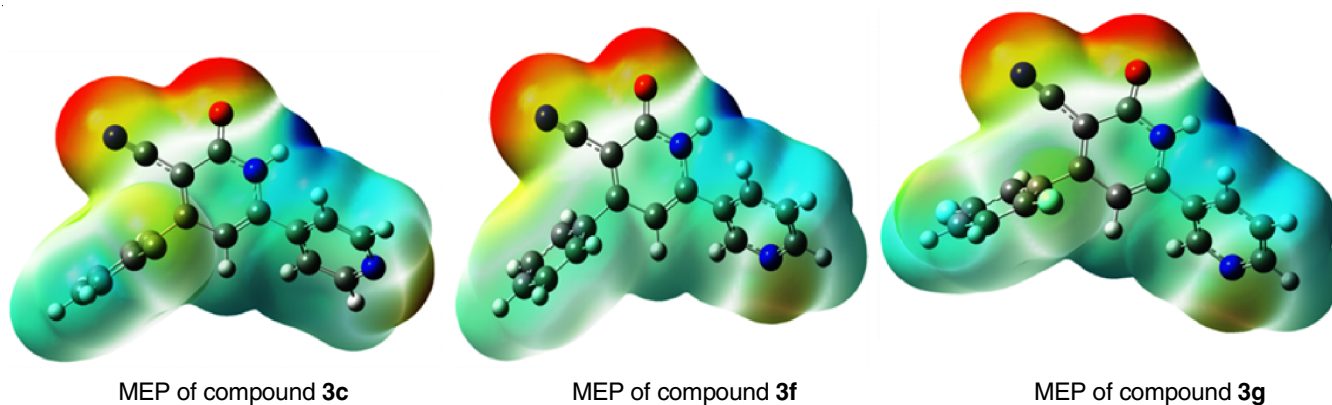
TABLE-3
BOND LENGTHS, BOND ANGLES AND DIHEDRAL ANGLES OF TOP THREE HIT COMPOUNDS (**3c**, **3f** AND **3g**)

Bond length (Å)		Bond angle (°)		Dihedral angle (°)	
Compound 3c					
H30-C17	1.08784	H30-C17-C8	119.963	H30-C17-C18-H31	-0.110
C17-C18	1.39365	C17-C18-H31	119.923	H30-C17-C18-C19	179.666
C18-H31	1.08773	C17-C18-C19	120.085	C17-C18-C19-H32	179.881
C18-C19	1.39668	H31-C18-C19	119.991	C17-C18-C19-C7	-0.373
C19-H32	1.08825	C18-C19-H32	118.845	H31-C18-C19-H32	-0.326
C19-C7	1.40402	C18-C19-C7	120.533	H31-C18-C19-C7	179.182
C7-C15	1.40596	H32-C19-C7	120.621	C18-C19-C7-C6	179.813
C15-C20	1.72872	C19-C7-C6	118.621	C18-C19-C7-C15	0.708
C15-C16	1.39798	C19-C7-C15	118.806	H32-C19-C7-C15	-179.793
C16-H29	1.08658	C7-C15-C20	121.702	C19-C7-C6-C5	85.834
C16-C17	1.39468	C7-C15-C16	120.378	C19-C7-C15-C20	179.570
C7-C6	1.48452	C20-C15-C16	117.920	C19-C7-C15-C16	-0.606
C6-C5	1.35808	C15-C16-H29	120.438	C7-C15-C16-H29	-179.531
C5-C21	1.42008	C15-C16-C17	120.107	C20-C15-C16-H29	0.300
C21-N22	1.16075	H29-C16-C17	119.454	C20-C15-C16-C17	18.000
C5-C4	1.49129	C16-C17-H30	120.028	C15-C16-C17-H30	-179.564
C4-O9	1.22039	C16-C17-C18	120.008	C15-C16-C17-C18	0.176
C4-C3	1.36853	C15-C7-C6	122.487	H29-C16-C17-H30	0.138
N3-H24	1.01184	C7-C6-C5	119.697	C16-C17-C18-H31	-179.631
N3-C2	1.37630	C6-C5-C21	125.099	C16-C17-C18-C19	-0.075
C2-C1	1.34923	C6-C5-C4	115.983	C16-C15-C7-C6	-179.675
C1-H23	1.08713	C5-C21-N22	177.686	C20-C15-C7-C6	0.501
C1-C6	1.47429	C21-C5-C4	118.916	C15-C7-C6-C5	-95.095
C2-C8	1.47409	C5-C4-O9	123.781	C7-C6-C5-C21	-0.298
C8-C14	1.39845	C5-C4-N3	120.553	C7-C6-C5-C4	-179.730
C14-H28	1.08507	O9-C4-N3	115.664	C6-C5-C21-N22	-11.818
C10-H25	1.08386	C4-N3-H24	117.736	C6-C5-C4-O9	178.119
C10-C8	1.39689	C4-N3-C2	122.389	C6-C5-C4-N3	-1.336
C14-C13	1.38457	H24-N3-C2	119.700	N22-C21-C5-C4	167.598
C13-H27	1.08672	N3-C2-C1	119.164	C21-C5-C4-O9	-1.350
C13-N12	1.34892	N3-C2-C8	119.941	C21-C5-C4-N3	179.195
N12-C11	1.34876	C2-C1-H23	121.587	C5-C4-N3-H24	176.546
C11-H26	1.08599	C2-C1-C6	121.115	C5-C4-N3-C2	1.377
C11-C10	1.38553	H23-C1-C6	117.280	O9-C4-N3-H24	2.951
		C1-C6-C7	119.519	O9-C4-N3-C2	-178.121
		C1-C6-C5	120.783	C4-N3-C2-C8	-179.458
		C1-C2-C8	120.882	C4-N3-C2-C1	-0.769
		C2-C8-C14	120.070	H24-N3-C2-C8	5.464

		C8-C14-H28	121.654	H24-N3-C2-C1	-175.846
		C8-C14-C13	118.555	N3-C2-C8-C14	50.832
		H28-C14-C13	119.785	N3-C2-C1-H23	-178.236
		C14-C13-H27	121.015	N3-C2-C1-C6	0.153
		C14-C13-N12	123.769	C2-C1-C6-C5	-0.201
		H27-C13-N12	115.216	H29-C16-C17-C18	179.879
		C13-N12-C11	116.791	C2-C1-C6-C7	-179.722
		N12-C11-H26	115.132	H23-C1-C6-C7	-1.266
		N12-C11-C10	123.807	H23-C1-C6-C5	178.254
		H26-C11-C10	121.061	C1-C6-C7-C15	84.431
		C11-C10-H25	119.740	C1-C6-C7-C19	-94.640
		C11-C10-C8	118.515	C1-C6-C5-C21	-179.817
		H25-C10-C8	121.742	C1-C6-C5-C4	0.751
		C10-C8-C14	118.561	C2-C8-C14-H28	1.422
		C10-C8-C2	121.360	C2-C8-C14-C13	-179.498
				C8-C14-C13-H27	-179.702
				C8-C14-C13-N12	0.325
				H28-C14-C13-H27	-0.604
				H28-C14-C13-N12	179.424
				C14-C13-N12-C11	-0.029
				H27-C13-N12-C11	179.997
				C13-N12-C11-H26	179.769
				C13-N12-C11-C10	-0.063
				N12-C11-C10-H25	179.238
				N12-C11-C10-C8	-0.584
				H26-C11-C10-C8	-179.969
				C11-C10-C8-C14	0.438
				C11-C10-C8-C2	179.401
				H25-C10-C8-C14	-178.934
				H25-C10-C8-C2	0.029
				C10-C8-C14-C13	-0.521
				C10-C8-C14-H28	-179.601
				C10-C8-C2-N3	-128.115
				C10-C8-C2-C1	53.218
Compound 3f					
H30-C17	1.08642	H30-C17-C18	119.939	H30-C17-C18-H31	-0.003
C17-C18	1.39483	C17-C18-H31	119.893	H30-C17-C18-C19	179.814
C18-H31	1.08753	C17-C18-C19	120.084	C17-C18-C19-H32	179.862
C18-C19	1.39579	H31-C18-C19	120.023	C17-C18-C19-C7	-0.529
C19-H32	1.08756	C18-C19-H32	118.959	H31-C18-C19-H32	-0.322
C19-C7	1.40076	C18-C19-C7	120.199	H31-C18-C19-C7	179.288
C7-C15	1.40142	H32-C19-C7	120.841	C18-C19-C7-C6	179.482
C15-H28	1.08745	C19-C7-C15	120.813	C18-C19-C7-C15	0.725
C15-C16	1.39589	C19-C7-C15	119.406	H32-C19-C7-C6	-0.916
C16-H29	1.08767	C7-C15-H28	120.677	H32-C19-C7-C15	-179.673
C16-C17	1.39369	C7-C15-C16	120.214	C19-C7-C15-H28	179.763
C7-C6	1.48068	H28-C15-C16	119.108	C19-C7-C15-C16	-0.477
C6-C5	1.35821	C15-C16-C17	120.075	C7-C15-C16-H29	-179.740
C5-C20	1.42007	C15-C16-H29	120.009	C7-C15-C16-C17	0.032
C20-N21	1.16138	H29-C16-C17	119.915	H28-C15-C16-H29	0.024
C5-C4	1.49215	C16-C17-H30	120.043	H28-C15-C16-C17	179.796
C4-O9	1.22011	C16-C17-C18	120.043	C15-C16-C17-H30	-179.565
C4-H23	1.01108	C16-C17-C18	120.018	C15-C16-C17-C18	0.169
N3-C2	1.37713	C15-C7-C6	119.769	H29-C16-C17-H30	0.207
C2-C1	1.34937	C7-C6-C5	120.002	H29-C16-C17-C18	179.942
C1-H22	1.08801	C6-C5-C4	115.947	C16-C17-C18-H31	-179.738
C1-C6	1.47515	N21-C20-C5	178.462	C16-C17-C18-C19	0.079
C2-C8	1.47138	C20-C5-C4	118.762	C16-C15-C7-C6	-179.247
C8-C10	1.39875	C5-C4-O9	123.825	H28-C15-C7-C6	0.992
C10-H24	1.08697	C5-C4-N3	120.620	C15-C7-C6-C5	-106.275
C10-C11	1.39390	C9-C4-N3	115.554	C7-C6-C5-C20	-0.111
C11-H25	1.08449	C4-N3-H23	119.687	C7-C6-C5-C4	179.638
C11-C12	1.38483	C4-N3-C2	119.677	C6-C5-C20-N21	-13.142
C12-H26	1.08623	N3-C2-C8	119.997	C6-C5-C4-N3	-1.583
C12-N13	1.34952	N3-C2-C1	119.076	N21-C20-C5-C4	167.115
N13-C14	1.35489	C2-C1-H22	121.717	C20-C5-C4-O90	-1.955
C14-H27	1.08765	C2-C1-C6	121.233	C20-C5-C4-N3	178.184

C14-C8	1.39380	H22-C1-C6	117.043	C5-C4-N3-H23	176.092
C4-N3	1.36874	C1-C6-C5	120.730	C5-C4-N3-C2	2.074
		C1-C6-C7	119.262	O9-C4-N3-H23	-3.780
		C1-C2-C8	120.813	O9-C4-N3-C2	-177.798
		C8-C10-C11	119.919	C4-N3-C2-C8	-179.743
		H24-C10-C11	119.260	C4-N3-C2-C1	-1.440
		C10-C11-C12	118.364	H23-N3-C2-C8	6.354
		H25-C11-C12	120.614	H23-N3-C2-C1	-175.343
		C11-C12-H26	121.068	N3-C2-C8-C10	50.094
		C11-C12-N13	123.640	N3-C2-C1-H22	-178.574
		H26-C12-N13	115.292	N3-C2-C1-C6	0.366
		C12-N13-C14	116.708	C2-C1-C6-C7	-179.07
		C12-N13-C14	116.708	C2-C1-C6-C5	0.013
		N13-C14-H27	114.164	H22-C1-C6-C7	-0.083
		N13-C14-C8	124.402	H22-C1-C6-C5	179.001
		H27-C14-C8	121.431	C1-C6-C7-C19	-105.936
		C14-C8-C10	116.964	C1-C6-C5-C20	-179.189
		C14-C8-C2	122.225	C1-C6-C5-C4	0.560
				C1-C6-C7-C15	72.817
				C6-C1-C2-C17	178.653
				H22-C1-C2-C8	-0.287
				C1-C2-C8-C10	-128.178
				C2-C8-C10-H24	1.244
				C2-C8-C10-C11	179.776
				C8-C10-C11-H25	-179.586
				H24-C10-C11-H25	-0.590
				H24-C10-C11-C12	179.257
				C10-C11-C12-N13	-179.886
				C10-C11-C12-N13	0.060
				H25-C11-C12-H26	-0.038
				H25-C11-C12-N13	179.907
				C11-C12-N13-C14	-0.053
				H26-C12-N13-C14	179.895
				C12-N13-C14-H27	179.175
				C12-N13-C14-C8	-0.594
				N13-C14-C8-C2	179.799
				H27-C14-C8-C2	-178.833
				H27-C14-C8-C2	0.371
				C14-C8-C2-N3	-129.081
				C14-C8-C2-C1	52.648
Compound 3g					
H31-C17	1.08582	H31-C17-C16	120.780	H31-C17-C18-F21	-0.316
C17-C18	1.39159	C17-C16-H30	120.754	H31-C17-C18-C19	179.956
C18-F21	1.33820	C17-C16-C15	119.488	C17-C18-C19-H32	179.896
C18-C19	1.39301	H30-C16-C15	119.757	C17-C18-C19-C7	-0.333
C19-H32	1.08630	C16-C15-F20	118.707	F21-C18-C19-H32	0.167
C19-C7	1.40038	C16-C15-C7	121.290	F21-C18-C19-C7	179.939
C7-C15	1.40300	F20-C15-C7	120.002	C18-C19-C7-C6	179.562
C15-F20	1.34087	C15-C7-C6	118.832	C18-C19-C7-C15	0.576
C15-C16	1.39269	C15-C7-C19	120.821	H32-C19-C7-C6	-0.673
C16-H30	1.08604	C7-C19-H32	121.602	H32-C19-C7-C15	-179.660
C16-C17	1.39394	C7-C19-C18	119.582	C19-C7-C15-C16	-0.407
C7-C6	1.48111	H32-C19-C18	118.815	C7-C15-C16-H30	-179.854
C6-C5	1.35821	C19-C18-F21	119.318	C7-C15-C16-C17	-0.019
C5-C22	1.41907	C19-C18-C17	121.306	F20-C15-C16-H30	0.388
C22-N23	1.16085	F21-C18-C17	119.376	F20-C15-C16-C17	-179.776
C5-C4	1.49231	C18-C17-H31	119.721	C15-C16-C17-H31	-179.782
C4-O9	1.21966	C18-C17-C16	119.499	C15-C16-C17-C18	0.271
C4-N3	1.36793	C15-C7-C6	120.339	H30-C16-C17-H31	0.052
N3-H25	1.01205	C7-C6-C5	119.877	H30-C16-C17-C18	-179.895
N3-C2	1.37711	C6-C5-C22	125.064	C16-C17-C18-F21	179.632
C2-C1	1.34888	C6-C5-C4	116.082	C16-C17-C18-C19	-0.097
C1-H24	1.0877	C5-C22-N23	177.199	C16-C15-C7-C6	-179.398
C1-C6	1.47563	C22-C5-C4	118.854	F20-C15-C7-C6	0.357
C2-C8	1.47102	C5-C4-O9	123.731	C15-C7-C6-C5	-103.169
C8-C14	1.39393	C5-C4-N3	120.493	C7-C6-C5-C22	-0.114
C14-H29	1.08626	O9-C4-N3	115.775	C7-C6-C5-C4	179.762

C14-C13	1.35441	C4-C3-C25	117.730	C6-C5-C22-N23	-8.628
C12-N13	1.35010	C4-N3-C2	122.425	C6-C5-CC4-O9	178.265
C12-H28	1.08600	H25-N3-C2	119.723	C6-C5-C4-N3	-1.492
N12-C11	1.38477	N3-C2-C1	119.156	N23-C22-C5-C4	171.499
C11-H27	1.08416	N3-C2-C8	119.956	C22-C5-C4-O9	-1.850
C11-C10	1.39412	C2-C1-H24	121.563	C22-C5-C4-N3	178.392
C10-H26	1.08741	C2-C1-C6	121.165	C5-C4-N3-H25	177.292
C10-C8	1.39896	H24-C1-C6	117.247	C5-C4-N3-C2	1.317
		C1-C6-C7	120.663	O9-C4-N3-N25	-2.484
		C1-C6-C5	119.449	O9-C4-N3-C2	-178.458
		C1-C2-C5	120.862	C4-N3-C2-C1	-0.600
		C2-C8-C14	122.214	C4-N3-C2-C8	-178.730
		C8-C14-H29	121.383	H25-N3-C2-C1	-176.496
		C8-C14-N13	124.431	H25-N3-C2-C8	5.373
		C14-N13-C12	116.684	N3-C2-C8-C10	51.135
		H28-C12-N13	115.289	N3-C2-C1-H24	-178.022
		N13-N12-C11	123.664	N3-C2-C1-C6	0.085
		N12-C11-H27	120.643	C2-C1-C6-C5	-0.355
		N12-C11-C10	118.339	C2-C1-C6-C7	-179.119
		H27-C11-C10	121.017	H24-C1-C6-C7	-0.932
		C11-C10-H26	119.270	H24-C1-C6-C5	177.832
		C11-C10-C8	119.928	C1-C6-C5-C4	-1.003
		H26-C10-C8	120.797	C1-C6-C5-C22	-178.873
		C10-C8-C14	116.953	C1-C6-C7-C19	-103.366
		C10-C8-C2	120.830	C1-C6-C7-C15	75.604
		C11-C12-H28	121.047	C1-C2-C8-C10	-126.963
		N13-C14-H29	114.182	C2-C8-C14-H29	0.470
				C2-C8-C14-N13	179.766
				C8-C12-N13-H28	179.961
				C8-C14-N13-C12	-0.147
				C6-C1-C2-C8	178.199
				C2-C8-C10-C11	-179.710
				C2-C8-C10-H28	1.122
				C8-C10-C11-H27	-179.615
				C8-C10-C11-C12	0.044
				H26-C10-C11-H27	-0.434
				H26-C10-C11-C12	179.224
				C10-C11-C12-H28	-179.917
				C10-C11-C12-N13	0.180
				H27-C11-C12-H28	-0.257
				H27-C11-C12-N13	179.840
				C11-C12-N13-C14	-0.131
				C12-N13-C14-H29	179.194
				N13-C14-C8-C10	0.354
				N13-C14-C8-C2	179.766
				H29-C14-C8-C2	0.470
				C14-C8-C2-N3	-128.254
				C14-C8-C2-C1	53.647

Fig. 4. Molecular electrostatic potential (MEP) map of **3c**, **3f** and **3g** compounds

confirms its highest capacity to accept electrons as well as it has the highest binding energy and inhibition constant in molecular docking studies. In compound **3c**, the HOMO and LUMO had leading contributions from a benzene ring. In compounds **3f** and **3g**, the HOMO and LUMO had leading contributions from the pyridyl ring and pyridone ring. In molecular docking studies, the pyridine and pyridone ring have more number of hydrogen bonding interaction, π -alkyl interaction, π - σ interaction. The frontier molecular orbitals of pyridylpyridone are shown in Fig. 3. Bond length, bond angle and a dihedral angle of compounds **3c**, **3f** and **3g** are given in Table-3.

Molecular electrostatic potential: The molecular electrostatic potential (MEP) map is one of the best computational methods which are used to predict the reactivity of the molecule and the biologically active site of the compound. Furthermore, it is an indicator of the reactivity regions of a target molecule. In Fig. 4, the red color indicates the nucleophilic sites and the blue color indicates the electrophilic sites. Particularly, the nucleophilic sites are more important because it is ready to make hydrogen bonding with protein. In synthesized compounds, **3c**, **3f** and **3g**, the negative potential was located in the region of carbonyl, cyano group and pyridine ring. Similarly, the most positive potential was located by the NH group of pyridone ring. These units would participate in non-covalent interactions with amino acid residues of enzymes (α -amylase enzymes) in molecular docking studies.

Conclusion

In summary, newly designed pyridylpyridone analogue was docked into the active site of α -amylase enzyme. To three hit molecules were selected, synthesized and investigated their experimental antidiabetic activity. The biological activities and binding regions were thoroughly identified with the help of DFT calculations. The selected compounds showed excellent results as expected. The present study is a focus to test the further biological studies of selected pyridyl pyridones.

ACKNOWLEDGEMENTS

The authors grateful to Biochemie Innovations Lab, Tindivanam, India for consultancy service during this research work.

CONFLICT OF INTEREST

The authors declare that there is no conflict of interests regarding the publication of this article.

REFERENCES

- S. Altürk, D. Avci, O. Tamer and Y. Atalay, *J. Mol. Struct.*, **1164**, 28 (2018); <https://doi.org/10.1016/j.molstruc.2018.03.032>
- Y. Ju and R.S. Varma, *J. Org. Chem.*, **71**, 135 (2006); <https://doi.org/10.1021/jo051878h>
- M. Radi, G.P. Vallerini, A. Petrelli, P. Vincetti and G. Costantino, *Tetrahedron Lett.*, **54**, 6905 (2013); <https://doi.org/10.1016/j.tetlet.2013.10.054>
- H. Hongo, R. Fujita, K. Watanabe, W. Ikeura and Y. Ohtake, *Heterocycles*, **53**, 2607 (2000); <https://doi.org/10.3987/COM-00-9020>
- J.L. Greene Jr. and J.A. Montgomery, *J. Med. Chem.*, **7**, 17 (1964); <https://doi.org/10.1021/jm00331a005>
- M.J. Gil, M.A. Manu, C. Arteaga, M. Migliaccio, I. Encio, A. Gonzalez and V. Martínez-Merino, *Bioorg. Med. Chem. Lett.*, **9**, 2321 (1999); [https://doi.org/10.1016/S0960-894X\(99\)00373-X](https://doi.org/10.1016/S0960-894X(99)00373-X)
- A.P. Krapcho, S.N. Haydar, S. Truong-Chiott, M.P. Hacker, E. Menta and G. Beggolini, *Bioorg. Med. Chem. Lett.*, **10**, 305 (2000); [https://doi.org/10.1016/S0960-894X\(99\)00689-7](https://doi.org/10.1016/S0960-894X(99)00689-7)
- G. Semple, B. Andersson, V. Chhajlani, J. Georgsson, M.J. Johansson, Å. Rosenquist and L. Swanson, *Bioorg. Med. Chem. Lett.*, **13**, 1141 (2003); [https://doi.org/10.1016/S0960-894X\(03\)00033-7](https://doi.org/10.1016/S0960-894X(03)00033-7)
- Y. Hamada, K. Kawachi, T. Yamamoto, T. Nakata, Y. Kashu, Y. Watanabe and M. Sato, *J. Cardiovasc. Surg.*, **42**, 159 (2001).
- A.P. Kozikowski and W. Tückmantel, *Acc. Chem. Res.*, **32**, 641 (1999); <https://doi.org/10.1021/ar9800892>
- P. Jagtap, F.G. Soriano, L. Virag, L. Liaudet, J. Mabley, E. Szabo, G. Hasko, A. Marton, C.B. Lorigados, F. Gallyas Jr., B. Sumegi, D.G. Hoyt, E. Baloglu, J. VanDuzer, A.L. Salzman, G.J. Southan and C. Szabo, *Crit. Care Med.*, **30**, 1071 (2002); <https://doi.org/10.1097/00003246-200205000-00019>
- D. Jochmans, J. Deval, B. Kesteleyn, H. Van Marck, E. Bettens, I. De Baere, P. Dehertogh, T. Ivens, M. Van Ginderen, B. Van Schoubroeck, M. Ehteshami, P. Wigerinck, M. Gotte and K. Hertogs, *J. Virol.*, **80**, 12283 (2006); <https://doi.org/10.1128/JVI.00889-06>
- Q. Xu, X. Jiang, W. Zhu, C. Chen, G. Hu and Q. Li, *Arab. J. Chem.*, **9**, 721 (2016); <https://doi.org/10.1016/j.arabjc.2015.08.001>
- D.I. Kuntz, *Science*, **257**, 1078 (1992); <https://doi.org/10.1126/science.257.5073.1078>
- J. Drews, *Science*, **287**, 1960 (2000); <https://doi.org/10.1126/science.287.5460.1960>
- G. Banupriya, R. Sribalan, V. Padmini and V. Shanmugaiyah, *Bioorg. Med. Chem. Lett.*, **26**, 1655 (2016); <https://doi.org/10.1016/j.bmcl.2016.02.066>
- R. Thomsen and M.H. Christensen, *J. Med. Chem.*, **49**, 3315 (2006); <https://doi.org/10.1021/jm051197e>
- F. Jensen, *Introduction to Computational Chemistry*, Wiley: Chichester, U.K. (1999).
- Y.D. Scherson, S.J. Aboud, J. Wilcox and B.J. Cantwell, *J. Phys. Chem.*, **115**, 11036 (2011).
- G. Banupriya, R. Sribalan and V. Padmini, *J. Mol. Struct.*, **1155**, 90 (2018); <https://doi.org/10.1016/j.molstruc.2017.10.097>
- S. Al-Zuhair, A. Dowaidar and H. Kamal, *J. Biochem. Technol.*, **2**, 158 (2010).
- S. Kathiresan, T. Anand, S. Mugesah and J. Annaraj, *J. Photochem. Photobiol. B*, **148**, 290 (2015); <https://doi.org/10.1016/j.jphotochem.2015.04.016>
- Y.-Y. Xu, Y. Cao, H. Ma, H.-Q. Li and G.-Z. Ao, *Bioorg. Med. Chem.*, **21**, 388 (2013); <https://doi.org/10.1016/j.bmc.2012.11.031>
- M.J. Frisch, G.W. Trucks, H.B. Schlegel, G.E. Scuseria, M.A. Robb, J.R. Cheeseman, J.A. Montgomery Jr., T. Vreven, K.N. Kudin, J.C. Burant, J.M. Millam, S.S. Iyengar, J. Tomasi, V. Barone, B. Mennucci, M. Cossi, G. Scalmani, N. Rega, G.A. Petersson, H. Nakatsuji, M. Hada, M. Ehara, K. Toyota, R. Fukuda, J. Hasegawa, M. Ishida, T. Nakajima, Y. Honda, O. Kitao, H. Nakai, M. Klene, X. Li, J.E. Knox, H.P. Hratchian, J.B. Cross, V. Bakken, C. Adamo, J. Jaramillo, R. Gomperts, R.E. Stratmann, O. Yazyev, A.J. Austin, R. Cammi, C. Pomelli, J.W. Ochterski, P.Y. Ayala, K. Morokuma, A. Voth, P. Salvador, J.J. Dannenberg, V.G. Zakrzewski, S. Dapprich, A.D. Daniels, M.C. Strain, O. Farkas, D.K. Malick, A.D. Rabuck, K. Raghavachari, J.B. Foresman, J.V. Ortiz, Q. Cui, A.G. Baboul, S. Clifford and J. Cioslowski, S.B. Tefanov, G. Liu, A. Liashenko, P. Piskorz, I. Komaromi, R.L. Martin, D.J. Fox, T. Keith, M.A. AlLaham, C.Y. Peng, A. Nanayakkara, M. Challacombe, P.M.W. Gill, B. Johnson, W. Chen, M.W. Wong, C. Gonzalez and J.A. Pople, *Gaussian 03, Revision C.02*, Gaussian, Inc., Wallingford, CT (2004).
- P.M. Sales, P.M. Souza, L.A. Simeoni, P.O. Magalhães and D. Silveira, *J. Pharm. Pharm. Sci.*, **15**, 141 (2012); <https://doi.org/10.18433/J3S53K>
- M.A. Jayasri, P.S. Unnikrishnan and K. Suthindhiran, *Pharmacogn. Mag.*, **11**, S511 (2015); <https://doi.org/10.4103/0973-1296.172954>
- M.H. Helal, S.A. El-Awdan, M.A. Salem, T.A. Abd-elaziz, Y.A. Moahamed, A.A. El-Sherif and G.A.M. Mohamed, *Spectrochim. Acta A Mol. Biomol. Spectrosc.*, **135**, 764 (2015); <https://doi.org/10.1016/j.saa.2014.06.145>
- S. Murugavel, N. Manikandan, D. Lakshmanan, K. Naveen and P.T. Perumal, *J. Chil. Chem. Soc.*, **60**, 3015 (2015); <https://doi.org/10.4067/S0717-97072015000300008>
- R. Parthasarathi, V. Subramanian, D.R. Roy and P.K. Chattaraj, *Bioorg. Med. Chem.*, **12**, 5533 (2004); <https://doi.org/10.1016/j.bmc.2004.08.013>